

Optimization Of Transesterification Of Beniseed Oil Catalysed By Thermally Activated Waste Bone

Oje Kanu Chukwu,^a, Ude Callistus Nonso,^{*b} Onukwuli Okechukwu Dominic,^c Babayemi A.^d, Elendu Collins C.,^e

(*callyjoe4real@gmail.com, +2348039353284)

^aProduction Department, Warri Refining & Petrochemical Company Ltd WRPC (Subsidiary of Nigerian National Petroleum Co-operation NNPC), Ekpan-Warri, Delta State, Nigeria.

^bDepartment of Chemical Engineering, Michael Okpara University of Agriculture, Umudike, Umuahia, Abia State, Nigeria.

^cDepartment of Chemical Engineering, Nnamdi Azikiwe University (NAU), Awka, Nigeria.

^{a,d}Chemical Engineering Department, Faculty of Engineering, Chukwuemeka Odumegwu Ojukwu University, Uli, Anambra State, Nigeria.

^eEngineering Research, Development and Production, Projects Development Institute (PRODA), Enugu State, Nigeria.

Abstract—Optimization of biodiesel produced from beniseed oil catalyzed by synthesized waste bone catalyst was studied. The catalyst was synthesized from waste cow bone by thermal activation at a temperature of 700 °C for 4 hour and characterized to determine its catalytic properties. The oil was extracted from the seed by solvent extraction with n-hexane and was characterized to determine its physiochemical properties. The biodiesel was produced and the process parameters such as methanol/oil molar ratio, reaction time, temperature, amount catalyst and agitation speed were optimized using response surface methodology (RSM). The results revealed that the beniseed yielded a good quantity of oil about 52 % and its properties showed that the waste bone catalyst was able to transesterify the oil without treatment. The process variables had significant effects on the yield and the optimum values of the variables are reaction time of 3 hours, reaction temperature of 60 °C, catalyst concentration of 3 w%, methanol/oil molar ratio 10:1 and agitation speed of 334 rpm with fatty acid methyl ester (FAME) yield of 94.60%. The properties of the biodiesel produced under optimized conditions met the ASTM standard and were within the acceptable limits.

Keywords—Biodiesel, Transesterification, Thermally activated waste bone, Beniseed oil, Optimization.

1. Introduction

Over the centuries ago, the world energy consumption has been on non-renewable fossil fuels. The overdependence on these fuel can lead to depletion and its shortage in near future. The combustion of these fuels emits gaseous pollutants that cause global warming and numerous environmental challenges. These aforementioned challenges associated with energy source from fossil fuel have continue to renew efforts in development of

alternative and renewable fuels. Biodiesel is one of the biofuels that has penetrated the world research in recent times (Onukwuli et al., 2017). This because of its outstanding properties such as renewability, biodegradability, non-toxicity, high flash point and good reduction in greenhouse emissions (Ude and Onukwuli, 2019a).

Conventionally, biodiesel is produced by chemical alkali or acid-catalyzed transesterification with methanol or ethanol in the presence of inorganic basic or acid catalysts as homogeneous reaction (Zhang et al., 2010). This method results in wastewater and treatment of alkaline wastewater generated after the reaction is difficult and environmental unfriendly. The byproduct glycerol needs to be separated and refined for further use.

In order to ameliorate these problems, development of heterogeneous catalysts was stimulated. The use of heterogeneous catalysts in biodiesel production has been widely accepted worldwide (Ude and Onukwuli, 2019a). They eliminate the additional processing costs associated with the use of homogeneous catalysts (Abebe et al. 2011; Galen et al., 2004). The application of affordable and natural heterogeneous catalysts can reduce the cost of biodiesel production. Numerous researchers have studied transesterification of vegetable oils using different heterogeneous catalysts. Veljkovic et al (2009) studied the kinetics of sunflower oil methanolysis catalyzed by calcium oxide. Onukwuli and Ude (2018) evaluated the kinetics of African pear seed oil (APO) methanolysis catalyzed by phosphoric acid-activated kaolin clay. Ude and Onukwuli (2019b) studied the African pear seed oil methanolysis catalyzed by thermally activated clay. Ulakpa et al. (2019) optimized the transesterification of neem seed oil catalyzed by waste goat bone. Different kind of materials commonly used for synthesis of heterogeneous catalysts are mollusk shell, eggshells, calcined fish scale, sheep bone, calcined bone etc (Viriya-Empikul et al., 2010; Ulakpa et al., 2019).

Among these materials, animal bone is one of the best solid wastes that is abundantly available worldwide. It has an improved catalytic properties when chemically or thermally activated (Ulakpa et al., 2019). It contains hydroxyapatite which makes it more porous with large surface area. The amount of waste bone required to transesterify vegetable oils is pertinent to determine to avoid mixing problem. This parameter alongside with other transesterification variables can be evaluated by optimization. This requires a large number of experiments and mathematical tool that can predict the effect of the variables of the reaction and their interactions. Therefore, this study focused on optimization of transesterification of beni seed oil catalyzed by waste cow bone using response surface methodology.

2. Materials and Methods

2.1 Materials

Beniseeds were bought from Ogbete Market Enugu, Enugu State, Nigeria while the waste bone was sourced from different restaurant and abattoirs in Enugu State Nigeria. The methanol, and other chemicals were all purchased from De-Cliff Integrated Services Ltd, Enugu, Nigeria and they are of analytical grade.

2.2 Methods

2.2.1 Extraction of oil from Beni seed.

2 kg of the Beniseed was measured using an analytical weighing balance into containers, pulverized to particle size of 900 μm using an industrial blender and soaked with 3 liters of n-hexane for two days. The containers were covered and made air tight to avoid evaporation of n-hexane. The solvent was separated from the oil using rotary vacuum evaporator (Laborota 4000) and was collected in the receiving flask. The oil which was remained in the sample flask was weighed after the process was completed (AOAC, 1990). The percentage yield of the oil was calculated as thus:

$$\% \text{ yield} = \frac{\text{weight of the oil extracted}}{\text{weight of the sample used}} \times 100 \quad (1)$$

2.2.2. Characterization of the Beni-seed Oil

The extracted oil from Beni-seed were characterized using appropriate AOAC (1990) for physiochemical properties and instrumentation such as Fourier Transform infra- red spectrometer (FTIR, Shimadzu FTIR-8400S) and gas chromatography mass spectrometer (GCMS, Thermo Finnigan Trace GC/Trace DSQ/A1300) for functional group and fatty acid profile respectively.

2.2.3 Preparation of the Catalyst

The sourced waste bones were soaked in boiling water for 8 hours at about 75 $^{\circ}\text{C}$ to remove tissues and fats in the bone and then rinsed with distilled water for 3-4 times to remove dust and impurities. The waste bones were dried in the drying oven at 110 $^{\circ}\text{C}$ for 4 hours to remove water and moisture before being ground finely to a < 2 mm particle size powder

using a hammer mill. The crushed and powdered catalysts were sieved using various mesh sizes (100-200) to get particle of uniform size of mesh screens. They were stored in a desiccator in the presence of silica and KOH pellets in order to avoid water and CO_2 (reaction with air) contact with the catalysts prior to further usage because the CaO catalyst will be reacted with CO_2 and converted into CaCO_3 , thus reducing its activity as a catalyst. The catalyst was activated by physical means (Thermal activation).

2.2.4 Synthesis of catalyst

The crushed/powdered waste bone was calcined in a muffle furnace at a temperature of 700 $^{\circ}\text{C}$ under static air with a heating rate of 10 $^{\circ}\text{C}/\text{min}$ for 4 hours to observe the influence of the calcination process on transformation of calcium species into hydroxyapatite and to remove any absorbed water. All calcined samples were stored in a desiccator in the presence of silica and KOH pellets in order to avoid water and CO_2 (reaction with air) contact with the catalysts prior to further usage.

2.2.5 Characterization of the catalyst

The synthesized catalyst was characterized to determine its morphology, elemental compositions, functional group, mineralogy and surface area using scanning electron microscope (SEM), X-ray fluorescence (XRF, ARL 9400XP), Fourier transform infra-red spectroscope (FTIR BUCK model M530), X-ray diffractometer (XRD) and Brunauer-Emmett-Teller (BET, ASAP 2020) respectively.

2.2.6 Transesterification Reaction

The oil sample was precisely quantitatively transferred into a flat bottom flask placed on a hot magnetic stirrer. Then specific amount of catalyst (by weight of oil sample) mixed with the required amount of methanol was added. The reaction flask was kept on a hot magnetic stirrer under constant temperature with defined agitation throughout the reaction. At the defined time, sample was taken out, cooled, and the biodiesel (i.e. the methyl ester in the upper layer) was separated from the by-product (i.e. the glycerol in the lower layer) by settlement overnight under ambient condition. The percentage of the biodiesel yield was determined by comparing the weight of layer biodiesel with the weight of oil used.

$$Y = \frac{\text{weight of biodiesel}}{\text{weight of oil used}} \times 100 \quad (2)$$

2.2.7 Design of experiment for transesterification of Beniseed oil catalyzed by heterogeneous catalysts.

Design Expert software (version 12) was used in this study to design the experiment and to optimize the reaction conditions. The experimental design employed in this work was a two-level-five factor fractional factorial design, including 32 experiments. Reaction temperature, catalyst concentration, methanol/oil molar ratio, reaction time and agitation speed were selected as independent factors for the optimization study. The response chosen was the

methyl ester yields obtained from transesterification of Beniseed oil. $2^5/2$ ($2^n/2$) factor fractional factorial experiments, $10(2n)$ axial points and 6 center points were carried out in order to predict a good estimation of errors and experiments were performed in a randomized order. The actual and coded levels of each factor are shown in Table 1 and design matrix with the response is presented in Table 2. Alpha is defined as a distance from the center point which can be either inside or outside the range, with the maximum value of $2^{n/4}$, where n is the number of factors. It is noteworthy to point out that the software uses the concept of the coded values for the investigation of the significant terms, thus equation in coded values is used to study the effect of the variables on the response. The empirical equation is represented as shown in Equation (3):

$$Y = \beta_0 + \sum_{i=1}^5 \beta_i X_i + \sum_{i=1}^5 \sum_{j=i+1}^5 \beta_{ij} X_i X_j + \sum_{i=1}^5 \beta_{ii} X_i^2 \quad (3)$$

Where Y is the predicted yield of FAME (%), X_i and X_j represent the transesterification process variables, β_0 is the offset term, β_i is the coefficient of linear (single) effect, β_{ij} is the coefficient of interaction effect and β_{ii} is the coefficient of quadratic effect.

Table 1: Experimental range and levels of independent process variables for biodiesel production.

Independent Variables	Units	Range and Level				
		$-\alpha$	-1	0	1	$+\alpha$
Molar Ratio (A)	mol/mol	6:1	8:1	10:1	12:1	14:1
Catalyst Concentration (B)	wt %	1.0	2.0	3.0	4.0	5.0
Temperature (C)	°C	45	50	55	60	65
Reaction time (D)	hr.	1	2	3	4	5
Agitation speed (E)	rpm	150	200	250	300	350

Table 2 Experimental design Matrix for the Transesterification studies.

Std	A:Methanol/ oil Molar Ratio (mol/mol)	B: Catalyst Concentration (wt%)	C:Temperature (°C)	D:Reaction time (h)	E:Agitation speed (rpm)	Biodiesel yield (%)
1	8	2	50	2	300	56
2	12	2	50	2	200	67
3	8	4	50	2	200	61
4	12	4	50	2	300	76
5	8	2	60	2	200	64
6	12	2	60	2	300	73
7	8	4	60	2	300	70
8	12	4	60	2	200	76
9	8	2	50	4	200	71
10	12	2	50	4	300	75
11	8	4	50	4	300	67
12	12	4	50	4	200	77
13	8	2	60	4	300	72
14	12	2	60	4	200	70
15	8	4	60	4	200	72
16	12	4	60	4	300	94
17	6	3	55	3	250	30
18	14	3	55	3	250	45
19	10	1	55	3	250	80
20	10	5	55	3	250	91
21	10	3	45	3	250	80
22	10	3	65	3	250	90
23	10	3	55	1	250	79
24	10	3	55	5	250	93
25	10	3	55	3	150	83
26	10	3	55	3	350	89
27	10	3	55	3	250	92
28	10	3	55	3	250	92
29	10	3	55	3	250	92
30	10	3	55	3	250	92
31	10	3	55	3	250	92
32	10	3	55	3	250	92

2.2.8 Characterization biodiesel

The properties of the produced biodiesel at optimal conditions were determined using ASTM D-6751. The determined properties of the biodiesel include: Acid value, FFA, saponification value, iodine value, density, viscosity, calorific value, flash point, cloud point, pour point and cetane number.

3. Result and Discussion

3.1 Oil yield

The percentage of oil extracted from beniseed is 52%. The observed oil yield of beniseed was found to be higher than the yields of some edible oil such as soybeans, 50% and cotton seed, 47% (Rashid *et al.*, 2009). The relatively high oil content of Beniseed will make it highly suitable and economical for industrial applications for FAME production, as any oil bearing seed that can produce up to 30% oil are regarded as suitable feedstock for FAME industrial production (Okolie *et al.*, 2012).

3.2 Characterization of oil

3.2.1 Physicochemical Properties of the oil

The summary of the physicochemical properties of the oil is presented in the Table 3. From the table, specific gravity has been described as one of the most basic and vital properties of the feedstock for FAME production (Alamu *et al.*, 2007) because of its correlation with cetane number, heating value feedstock storage and transportations (Ajav and Akingbehin 2002). The specific gravity obtained for Beniseed oil (BSO) lies within the standard range 0.87 – 0.98 for triglycerides (Alamu *et al.*, 2007). The acid value of Beniseed oil extracted for this work is 6.0mgKOH/g hence, the value indicates that it has good quality for biodiesel production. The result also reveal that the oil has moderate free fatty acid value of 3.0%. This value suggests pre-treatment step on the raw-oil before the transesterification step using homogeneous catalyst but the process could be avoided using heterogeneous catalysts. Saponification value of the feedstock was between the ranges of the standard 175 – 205 mgKOH/g oil (Okolie *et al.*, 2012). The Saponification values of BSO was found to be 184.3 mgKOH/g oil, this value indicates that the Beniseed is a normal triglyceride and suitable for FAME production. The physicochemical properties of the raw oil compare favorably with those of some other oils such as *Pongamiapinnata* (Agarwal & Garima, 2011), *Jatropha curcas* (Adebayo *et al.*, 2011), *Madhucaindica* (Azam *et al.*, 2005).

The density and high viscosity of the oil will make its atomization difficult in internal combustion engine, hence it cannot be used directly as bio-fuel. The low pour point shows that the oil will hardly solidify at room temperature hence can be stored for a long time. The oxidation stability of the oil was high and is good for production of biodiesel.

3.2.2 Fatty acid profile of BSO (GC –MS)

The summary of fatty acid compositions of BSO is presented in Table 4. From the table, it shows that the oil contained eight different main fatty acids: palmitic, stearic, oleic, Lignoceric, linoleic, Caproic, Lauric acid and Linolenic acid. Linoleic acid is the most abundant with 49.73% of the total fatty acid present. BSO summarily consist of 25.36% of saturated acids

(stearic acid, palmitic acid, Caproic acid, lauric acid and Lignoceric acid) and 74.64% unsaturated acids (oleic, linoleic, Linolenic acid,). The dominant unsaturated fatty acid of the oil was Linoleic acid, which accounted for 49.73% of the total fatty acid content, hence, the oil belongs to oleic acid category (Sonntag, 2012). The oleic acid content of BSO as reported in Table 4 is comparatively higher than 7-40% reported for coconut oil, palm oil and cottonseed oil (Ampaitopin *et al.*, 2006; Rashid *et al.*, 2009). This shows that BSO oil is highly unsaturated triglycerides. However, the fatty acid components of the BSO was found to be consistent with the fatty acids present in typical oils used for FAME production.

Table 4: Fatty acid composition of BSO oil.

Fatty acid	Structure	Composition (%)	Molecular weight (g/mol)
Caproic acid	C6:0	7.80	116.20
Stearic acid	C18:0	7.98	284.48
Palmitic acid	C16:0	5.89	256.4
Oleic acid	C18:1	24.54	304.470
Linoleic acid	C18:1	49.73	294.48
Lignoceric acid	C24:0	0.31	200.32
Lauric acid	C12:0	3.25	200.32
Linolenic acid	C18:3	0.37	368.63

3.2.3 Fourier Transform Infrared (FT-IR) Spectra Analysis of BSO

The FTIR spectrum of BSO was carried out and shown in Figure 1. From the result, obvious peaks of note were recorded. The region 723 cm^{-1} (679.61 cm^{-1} – 886.65 cm^{-1}) indicates the presence of =C-H(alkenes) functional groups. They possess bending type of vibrations appearing at low energy and frequency region in the spectrum and they are all double bounded. They are attributed to olefinic (alkenes) functional groups and are unsaturated. The characteristics peaks found in the region 1237 cm^{-1} (1050.15 – 1297.23 cm^{-1}) indicate stretching vibrations of C-O and C-O-C. They can also indicate the bending vibration of O-CH₃ in the spectrum (John *et al.*, 2000; Isah *et al.*, 2015).

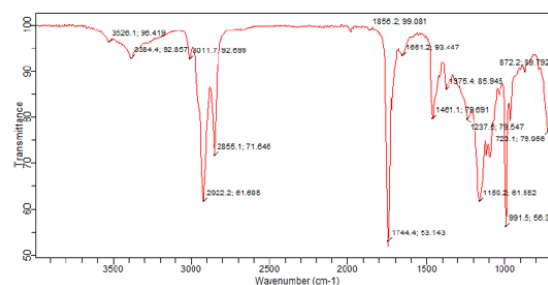


Figure 1: FT-IR spectra for BSO oil.

The band region of 1375 cm^{-1} can be ascribed to the bending vibration of C-H methyl groups, while the band at 1401 cm^{-1} ($1400\text{-}1800\text{ cm}^{-1}$) is ascribed to C=C bending vibrations (Shuit *et al.*, 2010). The peaks at 2855.75 cm^{-1} and 2922 cm^{-1} indicate symmetric and asymmetric stretching vibrations of C-H alkane groups respectively. They could be methyl (CH_3) or methylene groups and they require high energy to cause stretching vibrations within their bond when compared to the ordinary C-H bending vibrations of alkene groups detected at low energy and frequency region (Saifuddin *et al.*, 2014; Jimoh *et al.*, 2012). The peak at 3017 cm^{-1} and above is attributed to the stretching vibration of =C-H alkene groups. They are detected above wavenumber 3000 cm^{-1} in the spectrum compared to corresponding alkane C-H stretching groups detected below 3000 cm^{-1} .

3.3 Characterization of waste bone Catalyst

3.3.1 X-ray fluorescence (XRF) of waste bone catalyst

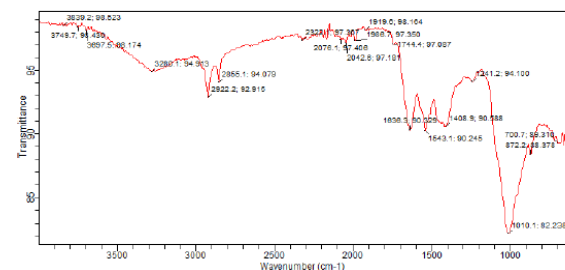
The study of the XRF elemental analysis of raw and thermal activated waste bone catalysts showed the presence of several elements as shown in Table 5. The calcium and phosphorous are the most abundant elements. The calcium content is higher in raw and lower in thermal activated waste bone. But the phosphorous content is higher in thermal activated waste bone. The presence of large amounts of calcium and phosphorous is compatible with the presence in abundance of calcium phosphate and carbonate.

Table 5: X-ray fluorescence (XRF) of waste bone catalysts.

Elements	Concentration (wt%)	
	Raw waste bone	Thermally activated waste bone
Na ₂ O	0.724	0.001
MgO	0.496	0.790
Al ₂ O ₃	1.177	0.550
SiO ₂	5.339	2.371
P ₂ O ₅	26.451	34.562
SO ₃	1.777	0.003
Cl	0.386	0.132
K ₂ O	0.341	0.380
CaO	61.076	59.951
TiO ₂	0.470	0.0083
Cr ₂ O ₃	0.000	0.000
Mn ₂ O ₃	0.005	0.001
Fe ₂ O ₃	1.467	0.129
ZnO	0.588	0.031
SrO	0.125	0.129

3.3.2 Fourier transforms infrared spectrometer of waste bone catalyst

Fourier transform infra-red (FTIR) spectroscopy of the raw waste bone and thermally modified waste bone catalysts were done to ascertain the functional groups present in them, the results are presented in Figures 2(a & b). The FTIR spectrum was scanned from $4000\text{-}400\text{ cm}^{-1}$. The presence of OH and PO₄ functional groups were confirmed by FTIR spectra. The peak appearing was assigned to various functional groups according to their respective wave numbers. From Figure 2a (raw waste bone), the broad bands at 1408.9 to 1642 cm^{-1} were attributed to adsorbed water, while sharp peak at 1919 and 2022 cm^{-1} were attributed to the stretching vibration of the lattice OH⁻ ions and the peak at 1100 cm^{-1} was assigned to the O-H deformation mode. The characteristic bands for PO₄³⁻ appear at 700.2 to 1261 cm^{-1} . The observation of the asymmetric P-O stretching vibration of PO₄³⁻ bands at 1241.2 cm^{-1} as a distinguishable peak, together with the sharp peak 1010.1 cm^{-1} correspond to the triply degenerated bending vibrations of PO₄³⁻ in hydroxyapatite.



can be attributable to the molecule $C = O$. The FTIR results were similar to those reported by Hengbo et al., (2007), Murugan et al., (2004) and Ghobadian et al., (2009).

3.3.3 Scanning Electron Microscopic (SEM) analysis

The SEM images for raw and thermally activated waste bones are presented in Figures 3(a & b). The figures show the surface morphology of waste bone catalyst taken at 1500x. The image shows a collapsed and rough surface covered with hair line cracks. The surface morphology taken have a tiny-hole-like surfaces that are specially designed to create a large number of pores that serve as the flow channels within the structure. 1500x magnification the surface morphology also shows a smooth-like surface. The morphology of the thermally activated waste bone as shown in Figure 3b, 1500x magnifications comprises irregular size and shape particles. The smaller size of the grains and aggregates could provide higher specific surface areas.

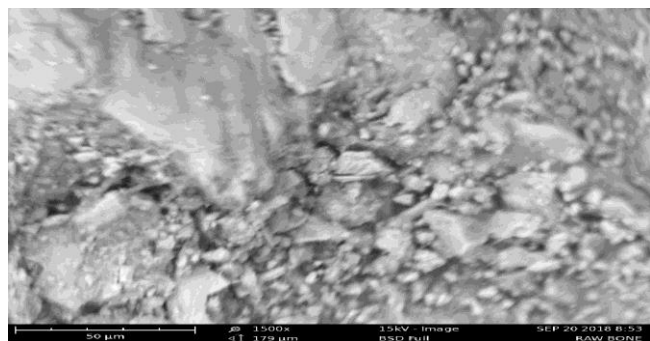


Fig. 3a: SEM images of raw waste bone at 1500x magnifications.



Fig.3 b: SEM images of thermally activated waste bone at magnifications 1500x.

3.3.4 X-ray diffraction of waste bone catalyst (XRD)

X-ray diffraction analysis was used to confirm the purity and stability of the raw, thermal and that of acid and base activated waste bones. It shows the diffraction angle or pattern of how the atoms are arranged in their crystals. Figure 4 (a & b) shows the XRD diffractograms of raw and thermally activated waste bone with the broad peak at 2θ . The

crystallography shows that the crystal system arrangement is hexagonal in nature.

The crystalline composition of waste bones for raw and thermally activated are similar with HAP pattern (JDS-Joint diffraction standard 00-009-0432) and the chemical reaction is $Ca_5(PO_4)_3(OH)$. In Figure 4a, the sample is with diffraction peak of 7° , 20° , 22° and 24° showing a poor crystallinity for raw waste bone. Also, the broadening and the overlapping of the diffraction peaks are due to the low crystal symmetry and crystal size of the bone mineral (Rogers et al., 2012; Eiden-Assmann et al., 2002). The morphology of the raw waste bone appeared like mass of aggregates, having less surface area.

In Figure 4b, it can be seen that the XRD pattern of thermally activated waste bone shows sharper peaks of 8° , 20° , 21° and 24° indicating better crystallinity. The peak positions for hydroxyapatite are in good agreement with the JCPDS (00-009-0432) and no pattern indicating the presence of impurities was observed. Therefore, standard hexagonal structure is formed. The crystallite size of the waste bone thermally activated was reduced. This shows that crystallinity of the waste bone decreased on thermal activation. It was also observed that the particle size reduction of the thermally activated waste bone spectra was maximum, exhibiting higher surface area, an important characteristic of a heterogeneous catalyst.

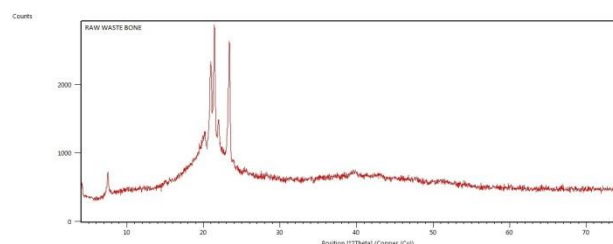


Fig. 4a: XRD pattern of raw waste bones.

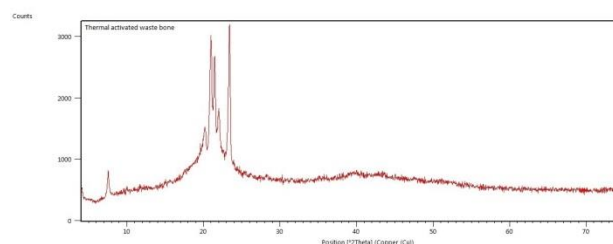


Fig. 4b: XRD pattern of Thermal activated waste bones

3.3.5 Brunauer- Emmet- Teller (BET) analysis of waste bone catalysts.

The textural properties (surface area, pore volume and pore size/diameter) of the raw waste bone and thermal activated waste bones were studied from N_2 adsorption isotherms using the method developed by

Brunauer- Emmett-Teller (BET). The results of the physical properties are summarized in Table 6.

Table 6: Surface area and porosity analysis of raw waste bone and thermal activated waste bone catalyst.

Sample name	Raw waste bone	Thermal activated waste bone.
Surface area (m ² /g)	11.234	97.34
Pore volume (cm ³ /g)	0.004	0.110
Pore size A ^o	5.901	1.672

The BET studies confirmed that higher surface areas and well-developed pore volume were obviously found on the surface of thermally activated waste bones compared to raw waste bone. The increase could be attributed to the destruction of the aliphatic and aromatic species and oxidation of the carbon by the activating agents (phosphoric acid-H₃PO₄ and sodium hydroxide-KOH) leading to swift removal of volatile matters during the activation process (Kongsuwan et al., 2009). The volatile matters include considerable organic by-products and minerals present in the activated waste bones surface. The increase in pore volume of the activated waste bones causes a less weight of the bones to occupy more space thereby leading to decrease in density. Chemical activation normally develops more porosity and gives high surface area and pore volume when compared with the raw (Ajayi et al., 2009).

3.4 Statistical analysis and optimization of biodiesel production

3.4.1 Statistical analysis of biodiesel production from BSO using Waste Bone Catalysts.

Design expert of response surface methodology version 12 was used to develop models for biodiesel production from Beniseed oil (BSO) using thermally activated bone waste. The design plan as shown in Table 2 and was used to optimize the yield of biodiesel production from BSO using thermal activated waste bone (TWB). The coded and uncoded values of the test variables were used to optimize the variables namely catalyst concentration, methanol/oil molar ratio, reaction temperature, reaction time and agitation speed. The experimental values of percentage yield were presented in Table 2. The models developed by the software are shown in Equation 4.

$$Y_{FAME(BSO)} \text{ by TWB } 76.38 + 1.29A + 0.4583B + 0.5417C + 0.2083D + 0.5417E$$

$$- 2.44AB + 1.19AC + 0.5625AD - 0.6875AE + 1.44BC - 0.9375BD + 0.5625BE - 2.06CD - 1.06CE + 0.81DE - 5.00A^2 - 4B^2 - 1.75C^2 - 2.88D^2 - 1.13E^2 \quad (4)$$

Where $Y_{FAME(BSO)}$ is the response of the variables (percentage yield of FAME) and A-E are the coded values of the independent variables. The above models represent the quantitative effect of the factors (A, B, C, D, and E) upon the response (Y). Equation 4 suggests that the yield of FAME has linear and quadratic effects on five variables studied. Coefficients with one factor represent the single effect of that particular factor while the coefficients with more than one factor represent the interaction between those factors. Positive sign in front of the terms indicates synergistic effect while negative sign indicates antagonistic effect of the factors. The adequacy of the above proposed model was tested using the Design Expert sequential model sum of squares and the model test statistics. From the statistical analysis, the predicted coefficient of determination, R² is in a reasonable agreement with the adjusted R² because the difference between them is less than 0.2. This test result is shown in Table 7.

Analysis of variance, ANOVA was applied to estimate the significance of the models at 5% significance level as shown in the Table 7. It could be observed that all the five variables: methanol/oil molar ratio (A), catalyst con.(B), reaction temperature (C), time (D) and agitation speed (E) have significant effect on yield of fatty acid methyl ester (FAME) produced by heterogeneous catalyzed reaction. Also from the result, it was clearly discovered that among the five variables studied for heterogeneous catalysis of activated waste bone, methanol /oil molar ratio (A) has the highest effect on the yield of FAME. There were also significant interaction effects between the variables studied; as shown by those between methanol/oil molar ratio and catalyst conc, methanol/oil molar ratio and temperature, methanol/oil molar ratio and agitation speed, methanol/oil molar ratio and time, catalyst concentration and reaction temperature, catalyst concentration and agitation speed, temperature and time, temperature and agitation speed, reaction time and agitation speed. The test of significance terms in the models as shown in Table 7 was carried out on 5% significance level. Individual terms in the model are said to be statistically significant to the responses if $P - val < 0.05$ and therefore, those statistically insignificant terms were eliminated from the model as shown in Equation 6.

$$Y_{FAME(BSO)} = 76.38 + 1.29A + 0.4583B + 0.5417C + 0.2083D + 0.5417E - 2.44AB + 1.19AC - 0.6875AE + 1.44BC - 2.06CD - 1.06CE + 0.81DE - 5.00A^2 - 4B^2 - 1.75C^2 - 2.88D^2 - 1.13E^2 \quad (6)$$

Table 7: Significance of regression coefficients of the yield of FAME Produced from BSO via TWB catalyst using the design-expert version 12

Source	Sum of Squares	Df	Mean Square	F-value	p-value	
Model	1661.21	20	83.06	66.85	< 0.0001	Significant
A-Methanol/ oil Molar Ratio	40.04	1	40.04	32.23	0.0001	
B-Catalyst Concentration	5.04	1	5.04	4.06	0.0001	
C-Temperature	7.04	1	7.04	5.67	0.0005	
D-Reaction time	1.04	1	1.04	0.8384	0.0002	
E-Agitation speed	7.04	1	7.04	5.67	0.0005	
AB	95.06	1	95.06	76.51	< 0.0001	
AC	22.56	1	22.56	18.16	0.0013	
AD	5.06	1	5.06	4.07	0.0686	
AE	7.56	1	7.56	6.09	0.0313	
BC	33.06	1	33.06	26.61	0.0003	
BD	14.06	1	14.06	11.32	0.0630	
BE	5.06	1	5.06	4.07	0.0686	
CD	68.06	1	68.06	54.78	< 0.0001	
CE	18.06	1	18.06	14.54	0.0029	
DE	52.56	1	52.56	42.31	< 0.0001	
A ²	733.33	1	733.33	590.24	< 0.0001	
B ²	469.33	1	469.33	377.76	< 0.0001	
C ²	89.83	1	89.83	72.30	< 0.0001	
D ²	242.46	1	242.46	195.15	< 0.0001	
E ²	37.13	1	37.13	29.88	0.0002	
Residual	13.67	11	1.24			
Lack of Fit	10.83	6	1.81	3.19	0.1121	

3.4.2 Predicted and actual values for yield of FAME from BSO via activated waste bone.

Analysis was also carried out on the experimental data in Table 2 to check the correlation between the experimental and predicted FAME yield from BSO catalysed by activated waste bone. The actual and predicted plot is shown in Figure 5. It could be seen from the figure that the data points on the plot were linearly distributed, indicating a good relationship between the experimental and predicted values of the response, and that the underlying assumptions of the above analysis were appropriate. The result also suggests that the selected quadratic model was proper and adequate in predicting the response variables for the experimental data.

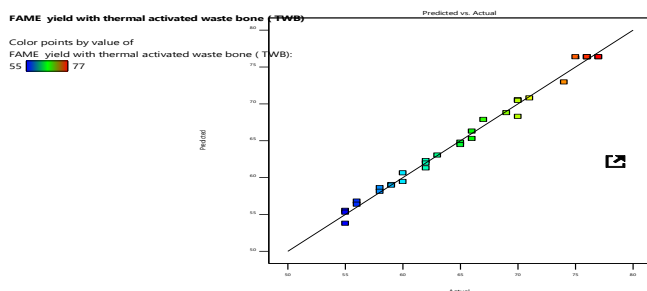


Figure 5: Plot of predicted values against the experimental values of FAME from BSO via TWB catalyst.

3.4.3 Optimization of FAME Production from BSO via waste bone catalyst using Desirability Function methods

The optimization of process variables in this study was carried out. FAME production from beniseed oil (BSO) using desirability function approach of response surface methodology in design expert. Desirability function approach eliminates the rigor associated with most other optimization techniques such as the optimization using contour and surface plots. It is a multi -response multi -factor optimization technique which operates on the principle established by Derringer Harrington. It optimizes a set of responses and defines the best factor settings for a solution of a multivariate objective function.

The optimal conditions are presented in Table 8. Therefore, it is seen from the table that the optimal yields of biodiesel or fatty acid methyl ester (FAME) 94.6% at optimized conditions as shown in Table 8.

Table 8 also depicts the validation of the optimal results of the transesterification process, from the table it could be observed that the percentage error of each response was less than 1%. This shows that the model was adequate in predicting the responses.

Table 8: Validation of the optimal values for BSO FAME via activated waste bone catalysis

S/N	Catalyst conc (wt%)	Methanol/oil molar ratio (mol/mol)	Temperature (°C)	Time (h)	Agitation speed (rpm)	Experimental Yield (%)	Predicted Yield (%)	% Error
1	3.0	10.2	60.2	3.2	334	95.03	94.60	0.45

3.4.5 Three dimensional surface plots for FAME yield from BSO via waste bone activated catalyst.

Figures 6 to 12 are the surface plots of the predicted FAME yield which can be generated by Equation (4) for the heterogeneous catalysis of BSO. The interaction effect of catalyst conc. and methanol/oil molar ratio on yield of FAME is shown in Figure 6. The figure show that the amount of methyl ester yield increases with methanol/oil molar ratio and catalyst concentration. However, at higher catalyst concentrations and methanol/oil molar ratio, a reduction in the yield can be observed due to the fact that the quadratic terms of the two factors are more significant with a negative effect.

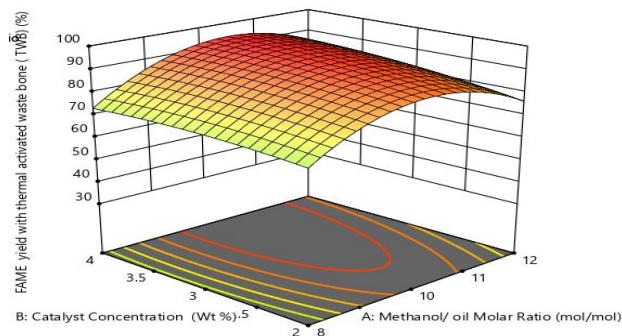


Figure 6: 3-D plots of catalyst conc. and methanol/oil molar ratio by TWB.

The interaction effect of methanol/oil molar ratio and reaction time on yield of FAME is depicted in Figure 7. The figure indicates that the amount of FAME yield increases with methanol/oil molar ratio and reaction time. This may be as a result of adequate time provided for conversion of the triglyceride. At higher methanol/oil molar ratio and reaction time, a drop in FAME yield can be observed due to the fact that the quadratic terms of the two factors are more significant with a negative effect.

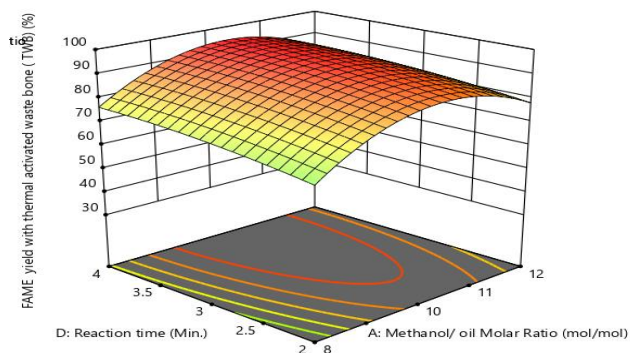


Figure 7: 3-D plots of reaction time and methanol/oil molar ratio by TWB.

The interaction effect of methanol/oil molar ratio and agitation speed on yield of FAME is presented in Figure 8. The figure shows that the FAME yield increases with methanol/oil molar ratio and agitation speed as a result of a positive significant effect of methanol/oil molar ratio and agitation speed interaction term on response. However, at higher methanol/oil molar ratio and agitation speed a reduction in the yield can be observed due to the fact that the quadratic terms of the two factors are more significant with a negative effect and the high speed could not allow further conversion of triglyceride.

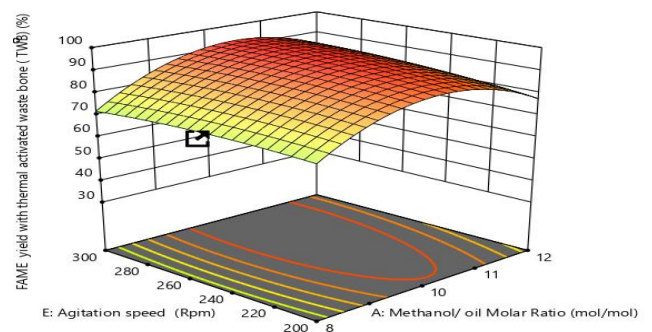


Figure 8: 3-D plots of agitation speed and methanol/oil molar ratio by TWB.

The interaction effect of catalyst conc. and temperature on yield of FAME is significant in all the catalyst used and shown in Figure 9. The figure indicates that the yield of FAME increases with reaction temperature and catalyst concentration. This is as a result of a positive significant effect of catalyst concentration and temperature interaction term BC as shown in (Eq. 4). However, at higher catalyst concentration and reaction temperature, a decrease in the yield can be observed due to evaporation of methanol at higher temperature and the fact that the quadratic terms of the two factors are more significant with a negative effect.

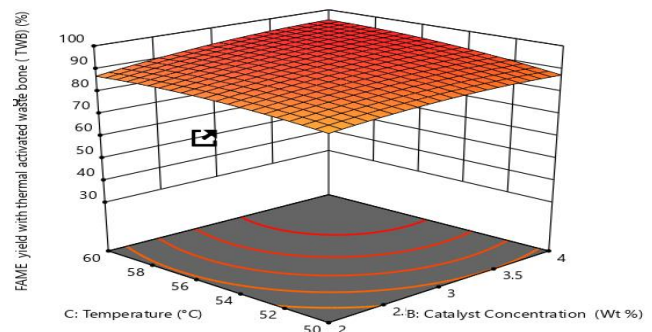


Figure 9: 3-D plots of temperature and catalyst concentration by TWB.

The interaction effect of catalyst conc. and agitation speed BE on yield of FAME is shown in Figure 10. The figure shows that the FAME yield increases with catalyst conc. and agitation speed which may be as a result of a proper mixing. However, at higher catalyst concentration and agitation speed a reduction in the yield can be observed due to the fact that the quadratic terms of the two factors are more significant with a negative effect and the high speed could not allow further conversion of triglyceride as seen in (Eq. 4).

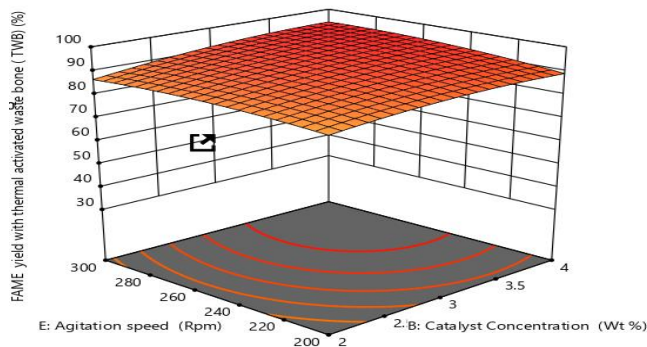


Figure 10: 3-D plots of agitation speed and catalyst concentration by TWB

The interaction effect of reaction temperature and agitation speed CE on yield of FAME is shown in Figure 11. The figure indicates that the yield of FAME increases with reaction temperature and agitation speed. However, at higher reaction temperature and agitation speed, there was a decrease in FAME yield because of the negative significant effect of reaction temperature-agitation speed interaction term, (CE) on response.

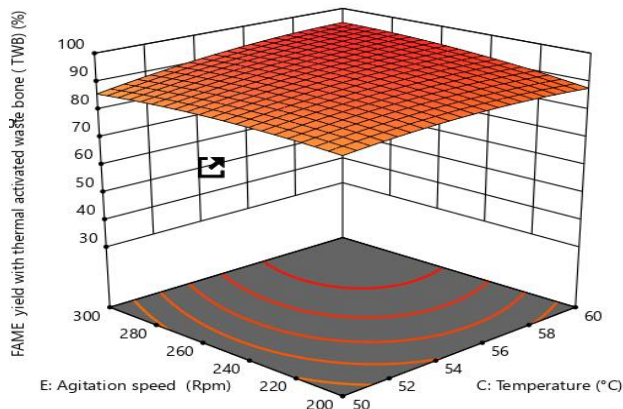


Figure 11: 3-D plots of agitation speed and temperature by TWB.

The interaction effect of time and agitation speed DE on yield of FAME is shown in Figure 12. The figure indicates that the yield of FAME increases with reaction time and agitation speed. However, at higher reaction time and agitation speed, there was a reduction in FAME yield which may be attributed to reversible reaction of transesterification resulting in loss of esters.

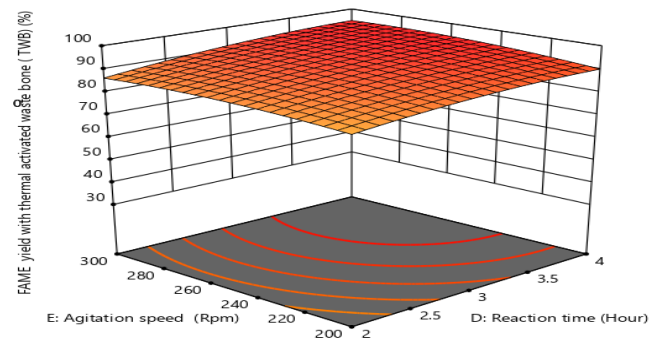


Figure 12: 3-D plots of agitation speed and reaction time TWB

3.5 Characterization of Biodiesel Produced using Optimal Conditions

The summary of all the fuel properties analyzed in the cause of this study was presented in Table 9, and the limits that they were compared with (ASTM D 6751 (2002) standards). The results of characterization of the produced FAME from BSO thermally activated catalysts. From the characterization result shown it can be seen that the properties of FAME are closely related to that given in American Standard for Testing Materials. Therefore, it can be used in a diesel engine.

Table 9: Fuel properties of BSO methyl esters compared with ASTM limits.

PROPERTY	UNITS	ASTM METHODS	BSO FAME by TWB	ASTM LIMITS
Density	kg/m ³	ASTM D-1298	866	830-880
Kinematics Viscosity	Cst	ASTM D-445	3.91	1.6-6.0
Flash Point	°C	ASTM D-93	170	≥130
Pour Point	°C	ASTM D-97	5	+15 max
Cloud Point	°C	ASTMD-2500	1.8	-15 to 5
Acid Value	mgKOH/g	ASTM D-974	0.18	≤ 0.80
Low Heating Value	MJ/kg		50.1	≥ 35
Aniline Point	(°C)	ASTM D-4737	176	
Higher Heating Value	MJ/Kg		62	
Oxidative stability	Hour	ASTM D-6751/EN 14112	6.1	3 min
Cetane number		ASTM D-130	54	47 min
Iodine Value	12/100g	ASTM D6751	49.02	120 Max

4. Conclusion

The optimization of FAME production from Beniseed oils using heterogeneous catalysts thermally activated waste bone (TWB) was carried out. It was established that the extracted oil yield from BSO using n-hexane solvent was within the quantity of oil obtained by some researchers. The low acid value, iodine value and saponification value of the oil enable it to undergo direct transesterification without treatment. The synthesized waste bone catalyst has good catalytic properties to catalyze the transesterification of BSO and the yield of FAME increased as process parameters increased to a reasonable point before it decreased. The optimum values of the parameters for BSO FAME are reaction time of 3 hours, reaction temperature of 60 °C, catalyst concentration of 3 w%, methanol/oil molar ratio 10:1 and agitation speed of 334 rpm. Under these conditions the amount of methyl ester yields achieved is 94.60 %. The properties of the biodiesel produced under optimized protocol in the present work meet the ASTM standard and were within the acceptable limits.

Reference

1. Abebe K, Endalew YK, Rolando Z (2011) Heterogeneous catalysis for biodiesel production from *Jatropha curcas* oil. *Energy* 36:2693–2700.
2. Adebayo, G.B, Ameen, O.M & Abass L.T. (2011). Physico-chemical properties of biodiesel produced from *Jatropha Curcas* oil and fossil diesel. *Journal of Microbiology and Biotechnology Research*, 1 (1), 12-16.
3. Agarwal, A.K & Rajamanoharan, K (2011) Experimental investigations of performance and emissions of Karanja oil and its blends in a single

cylinder agricultural diesel engine. *Applied Energy* 86(1): 106–112.

4. Ajav, E.A. & Akingbehin, A.O. (2002). A Study Of Some Fuel Properties Of Local Ethanol-Blended With Diesel Fuel; *Agricultural Engineering International; The CIGR Journal Of Scientific Research And Development*, Vol IV, Man A manuscript No. EE 01 003.

5. Ajayi, O. Adebayo, G.B, Ameen. (2009). The production of Methanol from Cow Dung. Paper presented at the Alternative Energy Conference: Options of Neccesity which held in Kuwait, Nov. 2 to 5. Organised by Kuwait Society of Engineers and World Federation of Engineering organizations. www.ec2009kuwait.org

6. Alamu, O.J., Waheed, M.A. & Jekayinfa, S.O. (2007). Biodiesel Production from Nigerian Palm Kernel Oil: Effect of KOH Concentration on Yield”, *Energy for Sustainable Development*, 11(3), 77-82.

7. Ampaitopin, S., Miyuki, K. & Tetsuo, T. (2006). Life cycle analysis of biodiesel fuel production: Case study of using used cooking oil as a raw material. Kyoto, Japan. *Proceeding 2nd Joint International Conference on Sustainable Energy and Environment*, SEE, 21-23. November 2006, Bangkok, Thailand.

8. AOAC (1990). Official Methods of Analysis, 15th edition, Association of Official Analytical Chemists. Washington DC.

9. ASTM, (2002). “Standard Specification for Biodiesel Fuel (B100) Blend Stock for Distillate Fuels”, American Society for Testing and Materials, D6751-02

10. Azam, M. M., Waris, A., Nahar, N, M. (2005). Prospects and potential of fatty acid methyl esters of

some non-traditional seed oils for use as biodiesel in India. *Biomass and Bioenergy*, 29, 293-302.

11. Eiden-Assmann, S. (2002). New Heavy Metal-Hydro-Sodalites Containing Cd^{2+} , Ag^+ or Pb^{2+} : Synthesis by Ion-Exchange and Characterization. *Material Resource Bulletin*, 37, 875–889. DOI:10.1016/S0025-5408(02)00715-8

12. Galen JS, Mohanprasad AD, Eric J, Duskocil PJM, Michael JG (2004) Transesterification of soybean oil with zeolite and metal catalysts. *Appl Catal A* 257:213–223.

Ghobadian, B., Rahimi, H., Nikbakht, A. M., Najafi, G. & Yusaf, T. F. (2009). Diesel engine performance and exhaust emission analysis using waste cooking biodiesel fuel with an artificial neural network. *Renewable Energy*, 34 (4), 976- 982.

13. Hengbo, Y., Lingqin, S., Aili, W., Yonghai, F., Yutang, S., Zhanao, W. & Tingshun, J. (2007). Liquid Phase Dehydration of Glycerol to Acrolein Catalyzed by Silicotungstic, Phosphotungstic, and Phosphomolybdic Acids, *Chemical Engineering Journal* 180, 277-300.

14. Isah, Y., Yousif, A.A., Feroz, K.K., Suzana, Y., Ibraheem, A. & Soh, A. C. (2015). Comprehensive characterization of napier grass as feedstock for thermochemical conversion. *Open Access Energies Journal*, 8: 3403-3417.

15. Jimoh, A., Abdulkareem, A.S., Afolabi, J.O. & Odigure Odili U.C. (2012). Production and characterization of biofuel from refined groundnut oil. 10–12.

16. John, C., Hosamani, K.M., Hiremath. (2000). Interpretation of infrared spectra, a practical approach. *Encyclopedia of analytical chemistry*, R.A. Meyers (Ed). John Wiley and Sons Ltd, Chichester. 10815–10837.

17. Kongsuwan, A., Patnukao, P. & Pavasant, P. (2009). Binary component sorption of Cu(II) and Pb(II) with activated carbon from *Eucalyptus camaldulensis* Dehn bark. *Journal of Industrial Engineering Chemistry*, 15,465–470

18. Murugan, S., Ramaswamy, M.C. & Nagarajan, G. (2004). Tyre pyrolysis oil as an alternate fuel for diesel engines, *SAE Paper*, 100, 200–2010.

19. Okolie, P.N., Egbenni, U. & Ajekwene, A.E. (2012). Extraction and quality evaluation of sandbox tree seed (*Hura crepitans*) oil. *World Journal of Agricultural Science*, 8,359–365

20. Onukwuli, D. O., Emembolu, L. N., Ude, C. N., Aliozo S. O., Menkiti M. C. (2017). Optimization of biodiesel production from refined cotton seed oil and its characterization. *Egyptian Journal of Petroleum* 26, 103–110.

21. Onukwuli OD, Ude CN (2018) Kinetic of African pear seed oil (APO) methanolysis catalyzed by

phosphoric acid-activated kaolin clay. *Appl Petrochem Res* 8:299–313.

22. Rashid, U., Farooq, A. & Gerhard, K. (2009). Evaluation of biodiesel obtained from cottonseed oil. *Fuel Processing Technology*, 90(9), 1157-1163.

23. Rogers, P. L., Chesterfield, D. M., Al-Zaini, E.O. & Adesoji, A. A. (2012). Production of biodiesel via ethanolysis of waste cooking oil using immobilised lipase. *Chemical Engineering Journal*. 207–208(1), 701-710.

24. Saifuddin, N. & Refai, H. (2014). Spectroscopy analysis of structural transesterification in biodiesel degradation. *Research Journal of Applied Sciences, Engineering and Technology*, 8(9), 1149–1159.

25. Sonntag, A. (2012). Reaction of fats and fatty acids. In: Balley (Eds) industrial oil and fat Products, fourth ed wiley, New York USA, 99-120.

26. Ude C. N., Onukwuli, O. D. (2019a) Kinetic modeling of transesterification of gmelina seed oil catalyzed by alkaline activated clay (NaOH/clay) catalyst. *Reaction Kinetics, Mechanisms and Catalysis*, 127:1039–1058.

27. Ude C. N., Onukwuli D., O., (2019b) African pear seed oil methanolysis catalyzed by thermally activated clay. *Journal of Engineering and Applied Sciences*, 15(1), 88-98.

28. Ulakpa W. C., Ude C. N., Ulakpa R. O. (2019) Optimization, kinetics and thermodynamics study of transesterification of neem oil using heterogeneous catalyst derived from waste of goat bones. *International Journal of Emerging Engineering Research and Technology* 7(9), 7-18.

29. Veljkovic, VB, Stamenkovic, OS, Todorovic, ZB, Lazic, ML& Skala, DU 2009,

'Kinetics of sunflower oil methanolysis catalyzed by calcium oxide' *Fuel*, vol. 88, pp. 1554-1562.

30. Viriya-Empikul, N., P. Krasae, B. Puttasawat, B. Yoosuk, N. Chollacoop, K. Faungnawakij, (2010). Waste shells of mollusk and egg as biodiesel production catalysts. *Bioresource Technol.* 101, 3765-3767.

31. Zhang L., Sheng B., Xin Z., Liu Q., Sun S. (2010) Kinetics of transesterification of palm oil and dimethyl carbonate for biodiesel production at the catalysis of heterogeneous base catalyst. *Bioresource Technology* 101, 8144-8150.